Modelling of CANDU Reactivity Devices with WIMS-AECL/MULTICELL and Superhomogenization

J.V. Donnelly[1], B.J. Min[2], E.V. Carruthers[1] and K. Tsang[1]

[1] Atomic Energy of Canada Limited
Sheridan Science and Technology Park
Mississauga, Ontario, L5K 1B2
[2] Korean Atomic Energy Research Institute

ABSTRACT

A method for the calculation of the three-dimensional neutron flux distribution in and around CANDU[a] reactor fuel channels and reactivity control devices has been developed. The method is based on one- and two-dimensional transport calculations with the WIMS-AECL lattice cell code, SPH homogenization, and three-dimensional flux calculations with finite-difference diffusion theory using the MULTICELL code. Numerical verification tests have shown good agreement with more rigorous calculations, and validation tests indicate good agreement with measured device properties.

[a] CANDU® is a registered trademark of Atomic Energy of Canada Limited

1 INTRODUCTION

The reactor physics analysis techniques used to represent reactivity control devices are an important component of CANDU reactor modelling, and comprise a portion of the present program for the validation of the WIMS-AECL lattice-cell [1, 2] for the application of that code to CANDU reactors. The modelling analysis of reactivity devices in CANDU reactors presents special challenges in reactor physics analysis. The significant features of CANDU reactivity devices relevant to their reactor physics analysis are

- The reactor physics analysis of movable reactivity devices in CANDU reactors is a three-dimensional problem that cannot be accurately approximated in two-dimensional geometry. This three-dimensional geometry is a result of the horizontal fuel channels and vertical reactivity devices in CANDU reactors. The geometric capabilities of the WIMS-AECL code allows explicit simulation of only one- and two-dimensional geometries.
- The behaviour of neutrons in and around the fuel and reactivity devices is accurately treated by neutron transport theory but not by standard diffusion theory.
- The behaviour of neutrons in the D_2O moderator far from the fuel and reactivity devices is modelled reasonably accurately by diffusion theory.

Although the use of three-dimensional neutron transport theory would seem to be a preferred method, the impact of performing explicit three-dimensional transport-theory analyses of these problems is very significant in terms of both computational and analyst effort. A three-dimensional transport-theory calculation using the DRAGON code [3] requires about 10 h of computation, whereas an equivalent diffusion-theory calculation requires about 1 min. The use of additional neutron transport codes beyond WIMS-AECL would necessitate their support and validation to a level similar to WIMS-AECL, for them to be equally qualified for application to the analysis of CANDU reactors.

One of the key approximations used in virtually all representations of CANDU reactivity devices is the separation of the analysis problem into (1) analysis of a three dimensional problem representing a unit cell

containing one or more fuel channels and a reactivity device, to determine the change in homogenized-cell properties caused by the deployment of the device, and (2) representing the reactivity device in the overall reactor core calculation by those incremental properties spread over one or more unit cells. This separation-of-variables approach is still considered to be a good approximation, although the detailed methodology of performing the required calculations is still an area of ongoing investigations.

This document describes the development and verification of a methodology for the analysis of CANDU reactivity devices based on

1. Use of WIMS-AECL for all neutron transport calculations in one or two dimensions,
2. Use of state-of-the-art homogenization theory to process multi-region flux distributions and cross sections calculated by WIMS-AECL into homogenized properties to be used in three-dimensional diffusion-theory calculations.
3. Use of conventional two-energy-group, finite-difference, three-dimensional diffusion theory for the neutron flux solution in models representing reactivity devices in a lattice of fuel channels, and
4. Representation of reactivity devices using incremental cross sections in the reactor core calculation.

2 METHODS USED IN WIMS-AECL CALCULATIONS

The lattice cell calculations reported in this document were performed using WIMS-AECL Version 2-4y [2], with the 89-energy group ENDF/B-V nuclear data library [1]. Within WIMS-AECL, either the two-dimensional Pij or the one-dimensional Perseus collision-probability neutron transport solutions were used in 33 neutron energy groups condensed from the 89 neutron energy groups in the nuclear data library.

The geometric models used to analyse the CANDU unit cells comprised of fuel, cladding, D_2O coolant, pressure and calandria tubes, and D_2O moderator represents the configuration in two dimensions. The geometry used in a typical 37-element unit cell model is presented in Figure 1. The fuel compositions used in these calculations are selected to be representative of the fuel in the actual environment of the reactivity device being analysed, and they are normally either fresh or mid-burnup UO_2 fuel.

The models used to represent reactivity devices in WIMS-AECL are designed to simulate those devices accurately in one- or two-dimensional geometry and provide representative environments of the devices. The basic features of these models are

- Reactivity devices are represented at the centre of the cell model with as much fidelity as is practical and required. For devices characterized by concentric annuli, one-dimensional annular geometry is used in WIMS-AECL; for devices with more complex two-dimensional characteristics, a two-dimensional collision probability solution is used within and near the device.
- Neighbouring fuel is represented by placing it in an annulus centred at the mean distance of fuel from the reactivity device, equal to $\sqrt{2}$ times the lattice cell pitch (= 20.205 cm for a standard CANDU lattice). The amount of fuel represented is equal to the inventory of four fuel channels, and the corresponding volumes of coolant and channel tubes are similarly conserved. The outer radius of the cell model encloses the total area of four unit cells (= 32.2434 cm for a standard CANDU lattice).
- Neighbouring fuel, clad and coolant are represented by a homogeneous region in the WIMS-AECL transport calculation.

3 ENERGY CONDENSATION

The WIMS-AECL calculations provide neutron flux distributions and cross sections in 33 energy groups for each region of the model. These quantities are condensed into two neutron energy groups for all following

[1] Unpublished Atomic Energy of Canada Limited Report

calculations. The two neutron energy groups are: group 1 ("fast") for neutron energies greater than 0.625 eV, and group 2 ("thermal") for neutron energies less than 0.625 eV. The condensed reaction cross sections in condensed group i in each region r and reaction x, $\Sigma_{r,x,i}$, are calculated to conserve reactions:

$$\Sigma_{r,x,i} = \frac{\sum_{k \in i} \phi^0_{r,k} \Sigma^0_{r,x,k}}{\sum_{k \in i} \phi^0_{r,k}} \tag{1}$$

where $\Sigma^0_{r,x,k}$ is the cross section for reaction x in group k in region r of the WIMS-AECL calculation.

x is "a" for absorption and "f" for fission

$\phi^0_{r,k}$ is the neutron flux in group k in region r of the WIMS-AECL calculation.

The condensed scattering cross sections in each region, $\Sigma_{r,s,i \to j}$, are calculated to conserve energy:

$$\Sigma_{r,s,i \to j} = \frac{\sum_{k \in i} \phi^0_{r,k} \sum_{l \in j} \Sigma^0_{r,s,k \to l}}{\sum_{k \in i} \phi^0_{r,k}} \tag{2}$$

The condensed transport cross sections in each region, $\Sigma_{r,t,i}$, are calculated to preserve leakage:

$$\Sigma_{r,t,i} = \frac{\sum_{k \in i} \phi^0_{r,k}}{\sum_{k \in i} \phi^0_{r,k} / \Sigma_{r,tr,k}} \tag{3}$$

The condensed neutron flux in each region, $\phi_{r,i}$, is calculated as follows:

$$\phi_{r,i} = \sum_{k \in i} \phi^0_{r,k} \tag{4}$$

4 HOMOGENIZATION

The homogenized properties of selected regions of the WIMS-AECL solution are calculated to form properties of the "cell-of-interest" for use in the MULTICELL [4] calculations. The equations used to form the homogenized properties of a set of regions t are

$$\Sigma_{x,i} = \frac{\sum_{r \in t} V_r \Sigma_{r,x,i} \phi_{r,i}}{\sum_{r \in t} V_r \phi_{r,i}} \tag{5}$$

$$\phi_i = \frac{\sum_{r \in t} V_r \phi_{r,i}}{\sum_{r \in t} V_r} \tag{6}$$

where V_r is the volume of region r.

All of the reactor core calculations discussed in this document were performed with the RFSP code [5], which does not currently treat up-scatter or non-thermal fissions. Therefore, the following calculations were

required to form the effective down-scatter cross section, Σ_m, from the net transfers between the fast and thermal groups and the effective thermal fission-yield cross section, $\nu\Sigma_f$, from total fast and thermal fission rates. The multigroup scattering and fission cross sections calculated by WIMS-AECL and MULTICELL are applied as follows:

$$\Sigma_m = \Sigma_{s,1\to 2} - \frac{\Phi_2}{\Phi_1}\Sigma_{s,2\to 1} \tag{7}$$

$$\nu\Sigma_f = \nu\Sigma_{f,2} + \frac{\Phi_1}{\Phi_2}\nu\Sigma_{f,1} \tag{8}$$

where Φ_i is the homogenized-cell flux in energy group i.

5 THE SPH HOMOGENIZATION METHOD

The starting point for any homogenization problem is an existing solution to the neutron flux distribution, normally from WIMS-AECL in the context of this document. The homogenization problem may be stated: how to determine uniform properties for a zone comprised of a heterogeneous group of regions in the existing solution such that another calculation using these uniform properties will result in a flux solution consistent with the original solution.

The neutron flux distribution near strong sources such as fuel or strong sinks such as absorbers may not be accurately calculated using homogenized-region diffusion theory (or some approximations to transport theory) when conventional homogenization theory as expressed in Equation 5 is used, as this method does not conserve both reactions and leakage. When conventionally homogenized cross sections are applied in a diffusion solution, the diffusion-theory solution may deviate from the original transport solution; these deviations are generally significant within a CANDU unit cell, especially when reactivity devices are present.

A method has been developed to define equivalent homogenized cross sections such that the solution of the homogenized problem will preserve the solution of the reference problem [6]. This technique has been called the "Superhomogénéization" method (SPH). Although the SPH method was originally developed for the homogenization of PWR fuel assemblies and sub-assemblies, the method is fully applicable to CANDU reactor problems as well. A significant benefit of the SPH method relative to some alternative homogenization techniques is that the transformed cross sections may be used in standard, unmodified homogenized diffusion or transport calculations.

In the SPH method, the solution to a homogenized-region flux calculation of the desired form is compared with the existing heterogeneous solution and iteratively improved according to the procedure developed by the SPH developers [6], until the two solutions are consistent.

The SPH method has been implemented in a computer code, REGAV, and calculates SPH factors $\mu_{r,i}$ for each energy group i and homogenized zone r. The cross sections are modified according to

$$\Sigma_{r,a,i} = \mu_{r,i}\Sigma_{r,a,i} \tag{9}$$

$$\Sigma_{r,s,i\to j} = \mu_{r,i}\Sigma_{r,s,i\to j} \tag{10}$$

$$\nu\Sigma_{r,f,i} = \mu_{r,i}\nu\Sigma_{r,f,i} \tag{11}$$

$$\Sigma_{r,tr,i} = \mu_{r,i}\Sigma_{r,tr,i} \tag{12}$$

As the number of degrees of freedom in the set of $\mu_{r,i}$ exceeds the number of reaction rates to be conserved, an additional condition must be applied to specify a unique solution [6]. A normalization condition is applied to conserve properties of the problem, normally the neutron flux in part or the whole of a cell. Two alternative normalization constraints have been implemented in REGAV:

- Flux-volume: the volume integral of neutron flux in each energy group of the total cell will be conserved. This is the simplest and default normalization.
- Unity SPH in one region: a single homogenized region can have SPH factors fixed at unity, and the group fluxes in that region will be normalized to the reference values. This normalization is the preferred method to be used in the moderator region of MULTICELL [4] calculations for CANDU applications so that a consistent flux definition is used in the moderator of all the homogenization calculations.

The process of calculating SPH-corrected homogenized-region cross sections begins with the preparation of a WIMS-AECL model. The WIMS-AECL model is used to calculate the multi-region neutron flux distribution and region-wise cross sections for this model. Next, the homogenization model is described to REGAV by specifying the set of regions of the WIMS-AECL solution for which equivalent homogenized properties are to be calculated. From this information, REGAV builds a one-dimensional model with homogenized region volumes equal to the sum of the volumes of the set of regions to be homogenized. Although the WIMS-AECL models may have represented the set of regions to be homogenized in one or two dimensions, the models and sets of regions to be homogenized are chosen to be transformable into one-dimensional geometry.

The homogenization solution depends on the method of solution and mesh discretization to be used in the homogenized problem, and so must be obtained by a similar method within the SPH calculation. The geometry simulated within REGAV is one-dimensional radial geometry, and the flux solution may use either mesh-centred finite-difference diffusion theory or collision-probability neutron transport theory.

To apply the SPH factors calculated in REGAV for one-dimensional radial geometry to the three-dimensional Cartesian geometry used in MULTICELL, it is necessary to preserve the effective mesh spacings in the two calculations. The overall scale of mesh spacings in each region can be controlled in the input to REGAV. So long as the mesh sizes in REGAV and MULTICELL are reasonably small compared with the mean-free-paths in the homogenized materials, the SPH factors will be relatively mesh-independent.

Although the SPH factors are calculated in one-dimensional radial geometry, and the final solution is in three-dimensions, the strongest gradients and heterogeneities (and, hence, effects requiring SPH factors) are in the radial direction relative to the fuel and devices; thus the calculated SPH factors should be quite applicable to the final solution geometry as well. The use of a single set of material properties (including SPH factors) in the three-dimensional problem may limit accuracies in highly heterogeneous CANDU reactor problems, as the spacing between the fuel and reactivity device varies continuously.

No problems were encountered in SPH convergence for CANDU-related problems. For some light-water-moderated configurations with more detailed energy-group structures, however, convergence problems have occurred, corresponding to configurations in which it appears to be impossible for diffusion theory to reproduce transport-theory results with any sets of properties.

6 TWO-ENERGY-GROUP FLUX SOLUTION IN MULTICELL

The neutron diffusion theory methods originally applied in the MULTICELL code include a number of features making that calculation consistent with the neutronic theory applied in POWDERPUFS-V (PPV) [7] and special methods developed for treating strong absorbers. These features include fissions in the thermal group only, no thermal-group to fast-group up-scattering, and the use of current-to-flux boundary conditions within the model. To perform calculations within MULTICELL consistent with WIMS-AECL and exploit the capabilities of WIMS-AECL and the SPH treatment, the following extensions were made to MULTICELL:

- Conventional finite-difference diffusion theory is used throughout the three-dimensional model; no internal boundary conditions are used. Although SPH-corrected cross sections are used in the model, they do not require special treatment within MULTICELL.
- Fissions are represented explicitly in both the fast and thermal energy groups.
- Up-scattering is represented from the thermal to the fast energy group.
- Conventional k and B^2 critical eigenvalue searches are performed.

The neutron flux equations solved in MULTICELL are now

$$\nabla[D_{r,1}(r)\nabla\Phi_1(r)] - [\Sigma_{r,a,1} + \Sigma_{r,s,1\to 2} + D_{r,1}B_c^2]\Phi_1(r) + \Sigma_{r,s,2\to 1}\Phi_2(r) + \frac{\nu\Sigma_{r,f,1}\Phi_1 + \nu\Sigma_{r,f,2}\Phi_2}{k} = 0 \quad (13)$$

$$\nabla[D_{r,2}(r)\nabla\Phi_2(r)] - [\Sigma_{r,a,2} + \Sigma_{r,s,2\to 1} + D_{r,2}B_c^2]\Phi_2(r) + \Sigma_{r,s,1\to 2}\Phi_1(r) = 0 \quad (14)$$

where $D_{r,i} = \dfrac{1}{3\Sigma_{r,tr,i}}$

The critical k eigenvalue is calculated

$$k = \frac{\sum_r V_r[\Phi_1(r)\nu\Sigma_{r,f,1} + \Phi_2(r)\nu\Sigma_{r,f,2}]}{\sum_r V_r[\Phi_1(r)(\Sigma_{r,a,1} + D_{r,1}B_c^2) + \Phi_2(r)(\Sigma_{r,a,2} + D_{r,2}B_c^2)]} \quad (15)$$

In the critical eigenvalue mode, $B_c^2 = 0$ and k is equal to k_∞. In the critical buckling mode, B_c^2 is solved such that $k = 1$. For the problems analysed in this document, the critical buckling solution was normally used as it is considered to best represent the conditions in a critical CANDU reactor core. The exception to this was in the numerical validation comparisons with MCNP [8], in which case the critical k eigenvalue was used.

Reflective boundary conditions were used in all MULTICELL calculations analysed in this document.

7 MODEL PREPARATION FOR MULTICELL

The preparation of a MULTICELL model is composed of

1. For each region of a MULTICELL model, a set of cross sections must be prepared from the results of WIMS-AECL calculations. A WIMS-AECL model is prepared for each zone of the MULTICELL model. In the calculations discussed in this document, three types of WIMS-AECL models were developed:
   - A "fuel region" model, consisting of fuel, cladding, coolant, and pressure and calandria tubes. During the SPH calculation for this region, the SPH factors in the moderator region are fixed at unity.
   - A "moderator" region. The moderator region was formed from a WIMS-AECL model identical to the "fuel region" model, and no SPH factors were applied to this material.
   - A "device" model, extending radially outward to the guide tube if present. During the SPH calculation for this region, the SPH factors in the moderator region between the device and the fuel region are fixed at unity.
2. Rectangularized models of fuel and reactivity devices are formed. Volume conservation is used to form square representations of the cylindrical devices consistent with the WIMS-AECL models.
3. Meshes are determined such that about 3 mesh intervals per diffusion length ($=1/\Sigma_{tr}$) are present throughout the model. The number of mesh intervals is limited to no more than three per centimeter.
4. The minimum value of the transport cross section in either energy group for any material is limited to $0.08\ \mathrm{cm}^{-1}$, as smaller numerical values result in unrealistic diffusion-theory flux solutions. The effect of this bounding is not considered significant in current applications, as it occurs only in voided regions, in which case the absorption effects within those regions are small.

The last three components of MULTICELL model preparation have been automated in a utility code, so that the user input, once the WIMS-AECL models have been prepared, is minimal. The SPH calculations implement approximations consistent with the items 3 and 4.

8 CANDU REACTIVITY DEVICE MODELS IN MULTICELL

The three CANDU reactivity devices studied in this document are stainless steel adjuster rods, Zone Control Units (ZCU), and Mechanical Control Absorber (MCA) rods. An adjuster rod is a movable device containing a neutron absorbing material such as stainless steel of the order of 30 g/cm along its length. A ZCU is a compartment in which the amount of light water may be varied, having about 100 cm^3 light water per centimeter length. A ZCU has stronger neutron absorption properties than adjuster rods. An MCA is a cylindrical device having much stronger neutron capture properties than the adjuster rods or ZCUs, having about 27 g/cm of cadmium along its length.

The MULTICELL models are 28.575 cm wide by 14.28575 cm deep by 24.765 cm high (1 lattice pitch × $\frac{1}{2}$ lattice pitch × $\frac{1}{2}$ bundle length), with the device at one edge and the fuel in the middle of the cell, oriented perpendicularly to the device, similar to that shown in Figure 2 (in which the fuel is oriented vertically).

Although all of the MULTICELL models discussed in this document are of dimensions 1 lattice pitch × $\frac{1}{2}$ lattice pitch × $\frac{1}{2}$ bundle length, the properties of the devices were derived by averaging over the half of the model containing the reactivity device to maintain consistency with the representation of the devices in the reactor core calculations. Other related homogenized-region representations of CANDU reactivity devices are possible but have not been considered in this document.

The results of MULTICELL for use in CANDU reactor core calculations are expressed in terms of incremental cross sections, defined as

$$\Delta\Sigma_x = \Sigma_{x,perturbed} - \Sigma_{x,reference} \tag{16}$$

where $\Sigma_{x,reference}$ is the cell-averaged cross section for reaction x when the device is in its undeployed or empty configuration and

$\Sigma_{x,perturbed}$ is the cell-averaged cross section for reaction x when the device is deployed or full.

9 NUMERICAL VERIFICATION TESTS OF WIMS-AECL/MULTICELL

9.1 Comparisons Between MULTICELL and WIMS-AECL

The results of MULTICELL calculations for the reference lattices containing only fuel and moderator regions, using SPH-corrected homogenized region cross sections derived from WIMS-AECL, were compared with the results of the original WIMS-AECL calculations. The results of the two calculations were found to be in excellent agreement, as expected.

9.2 Comparisons Between MULTICELL and 3DDT

The results of MULTICELL calculations were compared with the results of an independent diffusion-theory code, 3DDT [9]. The 3DDT code performs finite-difference, multigroup diffusion-theory calculations using techniques similar to those in MULTICELL, and therefore primarily provides a calculational, rather than physics, comparison. The results of the two calculations were found to be in excellent agreement when using the same cross-section data, as expected.

9.3 Comparison of WIMS-MULTICELL and MCNP

The results of WIMS/MULTICELL calculations were compared with those of the Monte Carlo neutron transport code MCNP [8] for the configuration of a stainless-steel tube adjuster rod adjacent to a fuel channel containing 28-element CANDU fuel. The results of those calculations are presented in Table 1. In this comparison, and all others in this document, reactivity differences are calculated in mk, defined as

$$\rho = 1000 \times \left(\frac{1}{k_{reference}} - \frac{1}{k_{perturbed}} \right) \quad (17)$$

The results in Table 1 indicate good agreement in the calculated reactivity change. The 2.3 mk discrepancy in absolute eigenvalue is considered very good agreement considering the differences in methods of calculation. No evaluation of the agreement of WIMS/MULTICELL and MCNP was made for other CANDU reactivity devices.

9.4 Comparison of WIMS-AECL/MULTICELL and DRAGON

To verify the diffusion-theory calculations performed in MULTICELL with SPH-corrected homogenized-region cross sections from WIMS-AECL, calculations were performed using the three-dimensional neutron transport capabilities of the DRAGON cell code [3]. The models used in DRAGON were constructed to be equivalent to the MULTICELL models, although the geometric capabilities in DRAGON required coarser spatial discretization and allowed the cylindrical structures to be represented explicitly. Homogenized-region cross sections to be used in DRAGON were derived from the same WIMS-AECL models as for the MULTICELL calculations. The SPH calculation in REGAV obtained the one-dimensional radial flux using transport theory with spatial discretizations analogous to those used in DRAGON, to be consistent with the solution in DRAGON. It should be noted that these DRAGON calculations only used cross sections calculated from WIMS-AECL results, rather than cross sections calculated internally within DRAGON.

The results of the WIMS-AECL/MULTICELL and WIMS-AECL/DRAGON calculations are presented in Table 2. Differences between incremental cross section can frequently by characterised by the differences in $\Delta\Sigma_{a,2}$, as a large fraction of the neutrons absorbed in these devices are thermal.

The results in Table 2 indicate that the incremental cross sections calculated for stainless steel adjuster rods are in very good agreement between MULTICELL and DRAGON (+0.3% agreement in $\Delta\Sigma_{a,2}$). For the Zone Control Units, the agreement is not quite as good as in the adjuster rod case (-0.8% agreement in $\Delta\Sigma_{a,2}$) but is still considered quite acceptable accuracy. For the MCAs, there is an appreciable discrepancy between the MULTICELL and DRAGON results (-15% discrepancy in $\Delta\Sigma_{a,2}$). The trend in worsening agreement between MULTICELL and DRAGON is consistent with the greater challenge to the SPH treatment and diffusion theory in MULTICELL with the stronger absorption and three-dimensional flux gradients associated with the MCAs. A number of the approximations involved in the WIMS-AECL/MULTICELL models of the MCAs were investigated, but none was found to change the fundamental discrepancy significantly.

The SPH values of the reactivity device regions used in the models above are presented in Table 3, for the cases of diffusion- and transport-theory flux solutions and the same mesh discretization in both cases. The SPH factors are closest to unity in the case of adjusters and furthest in the case of MCAs, as expected.

10 REACTIVITY-DEVICE MEASUREMENTS IN CANDU REACTORS

The primary method used to measure the reactivity worth of reactivity devices in CANDU reactors during commissioning measurements is by balancing the reactivity change induced by changes in the device configuration against changes in dissolved boron poison in the moderator. The absolute boron concentrations in the moderator may be measured chemically, or changes in concentrations may be computed from the addition of measured weights of B_2O_3. A boron coefficient of reactivity is calculated by performing two RFSP reactor core calculations, one using cross sections calculated in the lattice cell code with boron at a nominal concentration, and a second calculation with boron in the moderator increased by 1 ppm. This reactivity measurement method is normally used for measurements of ZCUs and groups of adjuster rods.

The accuracy of measuring reactivity changes by changes in moderator boron concentration change is limited by the accuracy of (1) the measurement of boron concentration (estimated to be about ± 0.001 ppm[2] when water samples are analysed chemically), (2) the accuracy of dilution calculations when B_2O_3 is added to the moderator (estimated to be about $\pm 5\%$), and (3) the boron coefficient calculation (estimated to be about

[2] 1 ppm = 1 g boron per 10^6 g water

2.5 to 5% from differences between the values calculated by PPV and those calculated by WIMS-AECL for typical CANDU reactor configurations).

The secondary method used to measure the reactivity worth of devices in CANDU reactors is by balancing changes in ZCU levels against changes in the configuration of other reactivity devices, such as single adjuster rods. The accuracy of this method of reactivity measurement is limited by (1) the accuracy of the ZCU fill level measurements (estimated to be typically about ±0.7% from self-consistency tests), and (2) the accuracy of the ZCU reactivity calibration.

When calculated device reactivity values are converted from ZCU-based reactivity changes to boron-based reactivity changes, the ZCU total reactivity worth discrepancy relative to boron is applied to the average device reactivity. The uncertainties in boron-based devices reactivities are approximated by adding the ZCU reactivity-rate reproducibility to the device uncertainty, after adjustment for the range of ZCU level change during the measurement. This adjustment is made assuming that the reproducibility of ZCU level changes measurements improve proportional to the change in ZCU level change.

For each adjuster and MCA rod reactivity worth calculation, three RFSP $k_{effective}$ calculations were performed: (1) all rods in their initial configuration, initial ZCU level, (2) single rod moved, initial ZCU level, and (3) single rod moved, final ZCU level. These three $k_{effective}$ values are combined to produce the calculated rod worth from the (1) the reactivity worth of the change in zone level ($= k_2 - k_3$) and (2) the reactivity worth of the rod motion ($= k_2 - k_1$).

All the reactor measurements were performed at near zero reactor power, under cold conditions, with boron added to the moderator to suppress excess reactivity. For the fresh fuel cases, up to about 10 ppm boron was present in the moderator, and, in the equilibrium-fuel measurements which were performed following long shutdowns, up to about 5 ppm boron was present in the moderator. As the changes in moderator boron concentrations were not large during the measurements, reactor core and reactivity device properties were calculated at nominal boron concentrations only.

In the following discussions, it should be noted that all values reported in units of mk are, at least in part, derived using calculated values. Only percent ZCU fills and boron concentrations are measured quantities.

10.1 Comparison with Pickering-A Unit 2 Measurements

Pickering-A Unit 2 commissioning measurements were made with an equilibrium-burnup fuel configuration after a long shutdown. The measured values of critical ZCU level as a function of boron reactivity are presented in Table 4 (only the values of equivalent boron reactivity were available and the boron reactivity coefficient used in that equivalence is not expected to be consistent with WIMS-AECL). The results indicate an accuracy in the total ZCU worth calculated using RFSP of +6.4%. Since equal amounts of boron were added between each critical ZCU level measurement, the reactivity changes should be nearly equal as well; thus the variation in calculated reactivity changes between critical ZCU level reflects the self-consistency of the critical ZCU level measurements. The variation in calculated reactivity changes between critical ZCU levels indicates a reproducibility of about ±9.1% in the measured reactivity changes during 11% changes in ZCU levels.

Measurements of the individual reactivity worth of the six stainless steel adjuster rods in the Pickering-A Unit 2 reactor were compared with WIMS-AECL/MULTICELL analyses and are presented in Table 5. Adjuster reactivity worths were measured by withdrawing single rods. The results indicate an average difference of $+7.9 \pm 6.5\%$ between calculated adjuster rod and ZCU reactivity worth, or an equivalent $-14.3 \pm 7.2\%$ in boron reactivity worth. The uncertainty value of ±7.2% was calculated as $\sqrt{6.5^2 + 3.0^2}$, in which 3.0 was calculated as the percentage accuracy in the ZCU level measurements during average changes in ZCU levels of 33%, given the measured reproducibility of ±9.1% during ZCU level changes averaging 11% as presented in Table 4.

10.2 Comparison with Pickering-A Unit 4 Measurements

Pickering-A Unit 4 commissioning measurements were made with a fresh fuel configuration. The measured values of critical ZCU level as a function of boron concentration are presented in Table 6. The reactivity

worth of boron in the moderator was calculated to be 7.20 mk/ppm and used to convert the changes in boron concentration to equivalent reactivities. The results indicate a difference in the total ZCU worth of -2%. The variation in calculated reactivity changes between critical ZCU levels indicates a reproducibility of about ±17% in the measured reactivity change during 10% changes in ZCU levels.

Measurements of the individual reactivity worth of the six stainless steel adjuster rods in the Pickering-A Unit 4 reactor were compared with WIMS-AECL/MULTICELL analyses and are presented in Tables 7 and 8. During the measurements presented in Table 7, adjuster rods were withdrawn sequentially in the order shown, and boron was added to the moderator to return the reactor to similar critical ZCU levels after each successive rod measurement. During the measurements presented in Table 8, individual adjuster rods were inserted singly into the core, while other rods remained withdrawn. The results in Table 7 indicate an average difference of -12 ± 4 % between calculated adjuster rod and ZCU reactivity worth, whereas those in Table 8 indicate an average difference of -8 ± 1%. The differences in results between these two sets of measurements and calculations are due to two factors in the sequential withdrawal measurement: (1) as more rods were withdrawn, the reactor flux distribution in the core was changing, resulting in increasing individual rod worths as fewer were left in the core, and (2) the increasing boron levels added variability to the measurement conditions. The single rod insertion reactivity measurements and analyses are considered more representative of calculational accuracy of the device representation than the sequential withdrawal measurements because of the fewer complications during the measurements and analyses.

10.3 Comparison with Wolsong-1 Phase-B Measurements

Measurements of the reactivity worth of the ZCUs, adjuster rods and MCA rods in the Wolsong-1 CANDU-6 reactor during Phase-B Commissioning (fresh fuel configuration) were analysed [10]. Table 9 presents the measured and calculated ZCU reactivity worths. The reactivity worth of boron was calculated with WIMS-AECL/RFSP to be equal to 7.851 mk per ppm boron, and used to convert the boron additions into equivalent reactivities. The results in Table 9 indicate that the calculated ZCU reactivity worths agree with an accuracy +14.1% of total reactivity worth. The variation in calculated reactivity changes between critical ZCU levels indicates a reproducibility of ±5.1% in the measured reactivity worth of 8% changes in ZCU level.

Measurements and analyses of the reactivity worth of adjuster rods relative to ZCU level changes are presented in Table 10. Adjuster reactivities were measured by withdrawing single rods. The results in Table 10 indicate that the calculated adjuster rod reactivity worths agree to within -17.9 ± 6.1% of the ZCU reactivity changes. When the ZCU reactivity calibration relative to boron in the moderator is considered, the adjuster rod reactivity worths agree to within -3.8 ± 7.9% of equivalent boron in the moderator. In Table 11 some symmetries in the measured and calculated adjuster rod worths are presented according to their locations in the core, providing further useful information:

- The measured values of symmetric adjuster rods agree typically to ±3%
- There appears to be a general trend of under-prediction of adjuster rod worth in the middle of the core and better agreement farther out in the core.

Measurements and analyses of the reactivity worth of the MCAs relative to ZCU level changes are presented Table 12. The results in Table 12 indicate that the calculated MCA reactivity worths agree to within -6.6 ± 3.0% of the ZCU reactivity changes, and within +6.9 ± 3.5% of the equivalent boron in the moderator.

10.4 Summary of Validation Results

A summary of the results of ZCU and adjuster rod reactivity comparisons with measurements is presented in Table 13. The summarized results indicate that there is a significant variability in the agreement between measured and calculated reactivity device worths depending on the reactor, and the methods of measurement. Overall, the agreement of ZCU total and level change reactivity rates with measured values are respectively 10% and ±10%, although measurement uncertainties could contribute uncertainties of ±5-10%. The agreement in the adjuster rod results is very dependent on the accuracy of the ZCU calibration and the particular reactor, but average to -8 ± 1% relative to the ZCU reactivity changes and +6 ± 3% relative to boron.

Although the results of only a single measurement of MCA reactivity worth was presented in this paper, those results indicate reasonable accuracy of -6.6 ± 3.0% relative to ZCU reactivity changes, and within +6.9 ± 3.5% of the equivalent boron in the moderator. Numerical benchmark comparisons between MULTICELL and DRAGON, however, indicate differences of about 15% in MCA property calculations.

11 CONCLUSION

A new method has been developed for the analysis of CANDU reactivity devices, based on WIMS-AECL transport calculations, SPH homogenization and MULTICELL diffusion calculations. In numerical verification tests, the results of this approach have been shown to be in good agreement with more detailed three-dimensional Monte Carlo and three-dimensional collision-probability transport calculations for adjuster rods and ZCUs. For mechanical control rods, however, the discrepancies are larger and suggest further study is required.

In validation comparisons with measurements in three CANDU reactors, calculated reactivity worths of adjuster rods, ZCUs and MCAs are in reasonable agreement with the measured values. The results indicate that there is a significant variability in the agreement between measured and calculated reactivity device worths in different reactors, and that the uncertainties resulting from the methods of experimental measurement are significant contributors to this variability.

REFERENCES

[1] J.R. ASKEW, F.J. FAYERS and P.B. KEMSHELL, "A General Description of the Lattice Code WIMS", Journal of the British Nuclear Energy Society, 4(4), 564, 1966.

[2] J.V. DONNELLY, "WIMS-CRNL: A User's Manual for the Chalk River Version of WIMS", AECL Report, AECL-8955, 1986.

[3] G. MARLEAU, A. HÉBERT and R. ROY, "DRAGON User's Guide Version 2.0", École Polytechnique de Montréal Report IGE-71E1, 1994.

[4] A.R. DASTUR and D.B. BUSS, "MULTICELL — A 3-D Program of the Simulation of Reactivity Devices in CANDU Reactors", AECL Report, AECL-7544, 1983.

[5] B. ROUBEN, "Overview of Current RFSP-Code Capabilities for CANDU Core Analysis", AECL Report, AECL-11402, 1996.

[6] A. HÉBERT and G. MATHIONNIÈRE, "Development of a Third-Generation Superhomogénéziation Method for the Homogenization of a Pressurized Water Assembly", Nuclear Science and Engineering, 115, 124-141, 1993.

[7] B. ROUBEN, "Description of the Lattice Code POWDERPUFS-V", AECL Report, AECL-11357, 1995.

[8] J.F. BRIESMEISTER, "MCNP - A General Monte Carlo N-Particle Transport Code" Los Alamos Laboratory Report LA-12625, 1993.

[9] J.C. VIGIL, "3DDT, A Three Dimensional Multigroup Diffusion-Burnup Program", Los Alamos Laboratory Report LA-4396, 1970.

[10] B.J. MIN and J.V. DONNELLY, "WIMS-AECL/MULTICELL Calculations with SPH for Wolsong-1 Reactivity Devices", Proceedings of the Korean Nuclear Society Spring Meeting, May 1996.

TABLE 1: WIMS/MULTICELL AND MCNP RESULTS FOR AN ADJUSTER ROD CELL

Method of Calculation	Reference Cell	With Adjuster	Reactivity Change (mk)
MCNP	1.11298 ± 0.00045	0.99710 ± 0.00024	-104 ± 0.51
WIMS/MULTICELL	1.10972	0.995388	-103.0

TABLE 2: MULTICELL AND DRAGON INCREMENTAL CROSS SECTIONS FOR CANDU REACTIVITY DEVICES (10^{-3} cm^{-1})

Method of Calculation	$\Delta\Sigma_{tr,1}$	$\Delta\Sigma_{tr,2}$	$\Delta\Sigma_{a,1}$	$\Delta\Sigma_{a,2}$	$\Delta\Sigma_m$	$\Delta\nu\Sigma_f$
MULTICELL Adjuster	1.169	1.680	0.01924	0.6335	-0.01977	0.1223
DRAGON Adjuster	1.095	1.764	0.02730	0.6316	-0.02344	0.0892
MULTICELL ZCR	18.4	124.8	0.1811	1.192	2.593	0.05509
DRAGON ZCR	21.9	136.6	0.2032	1.202	2.101	0.04786
MULTICELL MCA	1.313	3.736	0.1519	4.782	-0.06275	0.8875
DRAGON MCA	0.808	5.028	0.2049	5.594	0.00387	0.7023

TABLE 3: SPH VALUES FOR TYPICAL CANDU REACTIVITY DEVICES

Method of Calculation	Group 1	Group 2
Adjuster — Diffusion Theory	0.932	1.030
Adjuster — Transport Theory	0.921	1.045
ZCU — Diffusion Theory	0.808	1.064
ZCU — Transport Theory	0.749	1.016
MCA — Diffusion Theory	0.954	0.751
MCA — Transport Theory	0.948	0.775

TABLE 4: MEASURED AND CALCULATED PICKERING-A UNIT 2 ZCU REACTIVITY WORTH

Assumed Boron mk	Measured ZCU Fill (%)	RFSP Calculated Reactivity Change mk	Difference %	Assumed Boron Change mk	RFSP Calculated Incremental Change mk	Difference %
0	76.4	0.00				
0.44	63.0	0.44	+0.0	0.44	0.44	+0.0
0.88	51.2	0.89	+1.1	0.44	0.45	+2.3
1.32	41.0	1.32	+0.0	0.44	0.43	-2.3
1.76	29.3	1.86	+5.7	0.44	0.54	+23.
2.20	19.3	2.34	+6.4	0.44	0.48	+9.1
Average			+2.6 ± 2.8	0.44	0.47 ± 0.04	+6.4 ± 9.1

TABLE 5: MEASURED AND CALCULATED PICKERING-A UNIT 2 ADJUSTER ROD REACTIVITY WORTHS

Adjuster Rod	Initial ZCU Fill %	Final ZCU Fill %	ZCU Reactivity Worth mk	Adjuster Reactivity Worth mk	Difference %
AA-7	31.3	64.4	1.40	1.40	+0.0
AA-9	30.6	61.6	1.33	1.42	+6.8
AA-10	30.3	62.8	1.39	1.42	+2.2
AA-12	30.9	62.1	1.33	1.43	+7.5
AA-8	30.0	64.2	1.38	1.57	+13.8
AA-11	30.0	63.5	1.35	1.58	+17.0
Average			1.36 ± 0.03	1.47 ± 0.08	+7.9 ± 6.5%

TABLE 6: MEASURED AND CALCULATED PICKERING-A UNIT 4 ZCU REACTIVITY WORTH

Boron Concentration (ppm)	Boron mk	ZCU Fill (%)	Calculated Reactivity Change mk	Difference %	Incremental Boron Change mk	Calculated Incremental Change mk	Difference %
9.850	0.00	88.4	0.00				
9.906	0.40	74.3	0.41	+2.5	0.40	0.41	+0.0
9.963	0.81	65.0	0.72	-11.1	0.41	0.31	-24.
10.019	1.22	56.1	1.05	-13.9	0.41	0.33	-20.
10.076	1.63	45.0	1.53	-6.1	0.41	0.48	+17.
10.132	2.03	38.5	1.85	-8.9	0.40	0.32	-20.
10.189	2.44	29.3	2.33	-4.5	0.41	0.48	+17.
10.245	2.84	21.0	2.78	-2.1	0.40	0.45	+13.
				-6.3 ± 5.1		0.40 ± 0.07	-2.4 ± 17

TABLE 7: MEASURED AND CALCULATED PICKERING-A UNIT 4 ADJUSTER ROD REACTIVITY WORTHS BY SEQUENTIAL WITHDRAWAL

Adjuster Rod Withdrawn	Initial ZCU Fill %	Final ZCU Fill %	ZCU Reactivity Worth mk	Adjuster Reactivity Worth mk	Difference %
AA-7	21.0	46.3	1.37	1.08	-21.4
AA-12	31.3	54.9	1.17	1.02	-12.4
AA-9	29.6	60.3	1.50	1.35	-10.0
AA-10	30.5	58.1	1.37	1.22	-11.0
AA-8	29.3	71.9	1.91	1.70	-11.0
AA-11	20.9	73.0	2.26	2.08	-7.7
Average			1.50 ± 0.37	1.41 ± 0.39	-12.2 ± 4.3%

TABLE 8: MEASURED AND CALCULATED PICKERING-A UNIT 4 ADJUSTER ROD REACTIVITY WORTHS BY INSERTION

Adjuster Rod Inserted	Initial ZCU Fill %	Final ZCU Fill %	ZCU Reactivity Worth mk	Adjuster Reactivity Worth mk	Difference %
AA-7	73.5	35.5	1.54	1.43	-7.1
AA-12	73.7	34.5	1.59	1.44	-9.4
AA-9	73.5	34.6	1.58	1.44	-8.9
AA-10	73.5	35.1	1.56	1.43	-8.3
AA-8	72.6	20.2	2.42	2.20	-9.1
AA-11	71.3	20.1	2.38	2.21	-7.1
Average			1.85 ± 0.43	1.69 ± 0.40	-8.3 ± 1.0%

TABLE 9: MEASURED AND CALCULATED WOLSONG-1 ZCU REACTIVITY WORTH

Boron Concentration Change (ppm)	Boron Change mk	Initial ZCU Fill %	Final ZCU Fill %	Calculated Change mk	Difference %
0.0564	0.443	89.89	79.94	0.492	+11.1
0.0565	0.444	79.80	70.66	0.524	+18.0
0.0564	0.443	70.66	62.85	0.497	+12.2
0.0562	0.441	62.92	55.05	0.556	+26.1
0.0565	0.444	54.68	47.78	0.518	+16.7
0.0565	0.444	48.01	41.51	0.509	+14.6
0.0565	0.444	41.50	35.10	0.524	+11.8
0.0565	0.444	35.42	29.42	0.479	+7.9
0.0565	0.444	29.06	23.08	0.497	+11.9
0.0565	0.444	23.30	17.30	0.481	+8.3
0.0565	0.444	17.30	11.18	0.490	+10.4
0.621	4.879			5.567	+13.8 ± 5.1

TABLE 10: MEASURED AND CALCULATED WOLSONG-1 ADJUSTER ROD REACTIVITY WORTHS

Adjuster	Initial ZCU Fill %	Final ZCU Fill %	Calculated ZCU mk	Calculated Adjuster mk	Difference %
1	36.66	39.76	0.257	0.225	-12.5
2	36.58	44.62	0.655	0.541	-17.4
3	36.51	46.21	0.772	0.658	-14.8
4	36.42	42.34	0.483	0.341	-29.4
5	36.52	46.46	0.792	0.650	-17.9
6	36.40	44.84	0.675	0.533	-21.0
7	36.61	39.85	0.263	0.222	-15.6
8	36.63	40.12	0.287	0.259	-9.8
9	36.55	47.00	0.824	0.689	-16.4
10	36.50	50.05	1.051	0.883	-16.0
11	36.47	45.07	0.665	0.482	-27.5
12	36.19	49.39	1.023	0.874	-14.6
13	35.68	47.51	0.888	0.689	-22.4
14	36.38	40.10	0.303	0.261	-13.9
15	36.72	39.42	0.233	0.226	-3.0
16	36.63	44.56	0.644	0.539	-16.3
17	36.40	46.61	0.822	0.660	-19.7
18	36.68	42.68	0.490	0.346	-29.4
19	36.43	47.00	0.841	0.655	-22.1
20	36.47	44.56	0.669	0.533	-20.3
21	36.49	39.69	0.262	0.219	-16.4
Total			12.899	10.485	-17.9 ± 6.1

TABLE 11: WOLSONG-1 ADJUSTER ROD CALCULATIONAL ERRORS

+1.3	-3.6	-1.0	-15.6	-4.1	-7.2	-1.8
+4.0	-2.6	-2.2	-13.7	-0.8	-8.6	-0.1
+10.8	-2.5	-5.9	-15.6	-8.3	-6.5	-2.6

Diagram showing the results for three rows of seven rods, indicating % error in adjuster rod reactivity worth relative to boron.

TABLE 12: MEASURED AND CALCULATED WOLSONG-1 MCA REACTIVITY WORTHS

Rod	Initial ZCU Level %	Final ZCU Level %	Calculated ZCU mk	Calculated MCA mk	Difference %
CA1	57.68	30.07	2.17	2.09	-3.7
CA2	58.61	28.93	2.34	2.08	-11.1
CA3	58.00	30.26	2.05	2.09	-4.1
CA4	57.24	28.92	2.24	2.07	-7.6
Average			2.23 ± 0.07	2.08	-6.6 ± 3.0

TABLE 13: SUMMARY OF ZCU AND ADJUSTER COMPARISONS WITH MEASUREMENTS

Reactivity Measurement	Pickering-A Unit 2	Pickering-A Unit 4	Wolsong-1	Average
ZCU Total	+6.4%	-2.1%	+14.1%	+10.3 ± 5.4%
ZCU Rate	±9%	±16	±5%	±9%
Adjuster vs. ZCU	+7.9 ± 6.5%	-8.3 ± 1.0%	-17.9 ± 6.1%	-8.2 ± 0.9%
Adjuster vs. Boron	+14.3 ± 11.1%	10.4 ± 16%	-3.8 ± 7.9%	+3.4 ± 6.0%

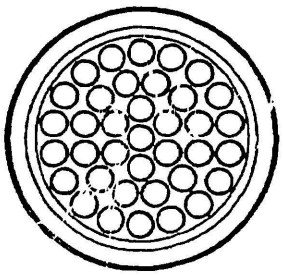

FIGURE 1: TYPICAL CANDU 37-ELEMENT UNIT CELL REPRESENTED IN WIMS-AECL

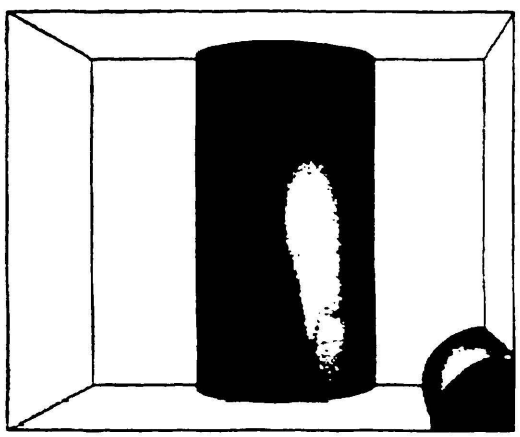

FIGURE 2: GEOMETRY USED IN MULTICELL REACTIVITY DEVICE MODELS